

Raman spectroscopy of halotrichite from Jaroso, Spain

Ray L. Frost ^{a*}, Matt L. Weier ^a, J. Theo Kloprogge ^a, Fernando Rull ^b

^aInorganic Materials Research Program, School of Physical and Chemical Sciences, Queensland University of Technology, GPO Box 2434, Brisbane Queensland 4001, Australia.

^bCristalografía y Mineralogía. Unidad Asociada al Centro de Astrobiología INTA-CSIC. Universidad de Valladolid. 47006, Valladolid, Spain, E-mail: rull@fmac.uva.es

This is the authors' version of a paper that was later published in: (2005) *Spectrochimica Acta* 62(1):pp. 176-180.
Copyright Elsevier

Abstract

Raman spectroscopy complimented with infrared ATR spectroscopy has been used to characterise a halotrichite $\text{FeSO}_4 \cdot \text{Al}_2(\text{SO}_4)_3 \cdot 22\text{H}_2\text{O}$ from The Jaroso Ravine, Almeria, Spain. Halotrichites form a continuous solid solution series with pickeringite and chemical analysis shows that the jarosite contains 6% Mg^{2+} . Halotrichite is characterised by four infrared bands at 3569.5, 3485.7, 3371.4 and 3239.0 cm^{-1} . Using Libowitzky type relationships, hydrogen bond distances of 3.08, 2.876, 2.780 and 2.718 Å were determined. Two intense Raman bands are observed at 987.7 and 984.4 cm^{-1} and are assigned to the ν_1 symmetric stretching vibrations of the sulphate bonded to the Fe^{2+} and the water units in the structure. Three sulphate bands are observed at 77 K at 1000.0, 991.3 and 985.0 cm^{-1} suggesting further differentiation of the sulphate units. Raman spectrum of the ν_2 and ν_4 region of halotrichite at 298 K shows two bands at 445.1 and 466.9 cm^{-1} , and 624.2 and 605.5 cm^{-1} respectively confirming the reduction of symmetry of the sulphate in halotrichite.

Key words: sulphate, halotrichite, jarosite, Raman spectroscopy

Introduction

Sulphate efflorescences have been known for some considerable time [1-3]. These often occur in tailings impoundments (see Jambour et al p322) [4]. The sulphate formation results from the oxidation of pyrite. Halotrichites are formed close to pyrite and are often found with copiapites and related minerals [5]. The minerals are found in efflorescences in geothermal fields [6]. Halotrichite is of formula $\text{FeSO}_4 \cdot \text{Al}_2(\text{SO}_4)_3 \cdot 22\text{H}_2\text{O}$ and forms an extensive solid solution series with pickeringite $\text{MgSO}_4 \cdot \text{Al}_2(\text{SO}_4)_3 \cdot 22\text{H}_2\text{O}$ [6-9]. The minerals are related to the alums $\text{R}_2\text{SO}_4 \cdot \text{M}_2(\text{SO}_4)_3 \cdot 24\text{H}_2\text{O}$ or $\text{RM}(\text{SO}_4)_2 \cdot 12\text{H}_2\text{O}$ where R represents an atom of a univalent ion such as ammonium, lithium, sodium, potassium and cesium and where M represents a trivalent metal such as aluminium, iron, chromium, gallium,

* Author to whom correspondence should be addressed (r.frost@qut.edu.au)

manganese, cobalt, rhodium and trivalent thallium. When a divalent atom is introduced instead of the monovalent atom, such as manganese, ferrous iron, cobalt, zinc and magnesium will form double sulphates. These sulphates form the halotrichites mineral series. These minerals are not isomorphous with the univalent alums. The minerals are all isomorphous and crystallise in the monoclinic space group $P2_1/c$. In the structure of the pseudo-alums, four crystallographically independent sulphate ions are present [10]. One acts as a unidentate ligand to the M^{2+} ion, and the other three are involved in complex hydrogen bond arrays involving coordinated water molecules to both cations and to the lattice water molecules.

Ross reports the interpretation of the infrared spectra for potassium alum as ν_1 , 981 cm^{-1} ; ν_2 , 465 cm^{-1} ; ν_3 , 1200, 1105 cm^{-1} ; ν_4 , 618 and 600 cm^{-1} [11]. Water stretching modes were reported at 3400 and 3000 cm^{-1} , bending modes at 1645 cm^{-1} , and librational modes at 930 and 700 cm^{-1} [12]. In the structure of alums, six water molecules surround each of the two cations. This means the sulphate ions are distant from the cations and coordinate to the water molecules. Ross also lists the infrared spectra of the pseudo-alums formed from one divalent and one trivalent cation. Halotrichite has infrared bands at ν_1 , 1000 cm^{-1} ; ν_2 , 480 cm^{-1} ; ν_3 , 1121, 1085, 1068 cm^{-1} ; ν_4 , 645, 600 cm^{-1} . Pickeringite the Mg end member of the halotrichite-pickeringite series has infrared bands at ν_1 , 1000 cm^{-1} ; ν_2 , 435 cm^{-1} ; ν_3 , 1085, 1025 cm^{-1} ; ν_4 , 638, 600 cm^{-1} [11]. These minerals display infrared water bands in the OH stretching, 3400 and 3000 cm^{-1} region; OH deformation, 1650 cm^{-1} region; OH libration, 725 cm^{-1} region. Ross also reports a weak band at ~ 960 cm^{-1} which is assigned to a second OH librational vibration [11]. As with the infrared spectra, Raman spectra of alums are based on the combination of the spectra of the sulphate and water. Sulphate typically is a tetrahedral oxyanion with Raman bands at 981 (ν_1), 451 (ν_2), 1104 (ν_3) and 613 (ν_4) cm^{-1} [13]. Some sulphates have their symmetry reduced through acting as monodentate and bidentate ligands [13]. In the case of bidentate behaviour both bridging and chelating ligands are known. This reduction in symmetry is observed by the splitting of the ν_3 and ν_4 into two components under C_{3v} symmetry and into 3 components under C_{2v} symmetry.

In this work we report the Raman and infrared spectra of a halotrichite from Jaroso, Spain.

Experimental

Minerals

The minerals used in this study were supplied by one of the authors (FR). The mineral halotrichite originated from Jaroso, Spain. The minerals were analysed by X-ray diffraction for phase purity and by electron probe using energy dispersive techniques for quantitative chemical composition.

Raman spectroscopy

The crystals of halotrichite were placed and oriented on the stage of an Olympus BHSM microscope, equipped with 10x and 50x objectives and part of a

Renishaw 1000 Raman microscope system, which also includes a monochromator, a filter system and a Charge Coupled Device (CCD). Raman spectra were excited by a HeNe laser (633 nm) at a resolution of 2 cm^{-1} in the range between 100 and 4000 cm^{-1} . Repeated acquisition using the highest magnification was accumulated to improve the signal to noise ratio. Spectra were calibrated using the 520.5 cm^{-1} line of a silicon wafer. In order to ensure that the correct spectra are obtained, the incident excitation radiation was scrambled. Previous studies by the authors provide more details of the experimental technique [14-17]. Spectra at elevated temperatures were obtained using a Linkam thermal stage (Scientific Instruments Ltd, Waterfield, Surrey, England). Spectral manipulation such as baseline adjustment, smoothing and normalisation was performed using the GRAMS® software package (Galactic Industries Corporation, Salem, NH, USA).

Results and discussion

The infrared spectrum and the Raman spectrum of halotrichite at 298 and 77 K in the $850\text{ to }1200\text{ cm}^{-1}$ region are shown in [Figure 1](#) and the results of the spectral analyses reported in [Table 1](#). The infrared spectra are broad but show two low intensity bands at 981.0 and 992.7 cm^{-1} . In the Raman spectra at 298 K an intense band is observed at 984.4 cm^{-1} with a shoulder at 987.7 cm^{-1} . In the 77 K spectrum of halotrichite two intense bands are observed at 991.3 and 1000.0 cm^{-1} with a third band at 985 cm^{-1} . These bands are sharp in comparison with the infrared bands. These bands are assigned to the ν_1 symmetric stretching mode of the SO_4^{2-} units. In the crystal structure of the pseudoalums there are four independent sulphate units, with one sulphate unidentate bonding to the divalent cation and the other three to the water molecules. Thus spectroscopically two symmetric stretching bands would be predicted and this is what is found in the 298 K Raman spectrum. The ratio of the intensities of the $984.4/987.7\text{ cm}^{-1}$ bands is approximately 25%. These values would suggest the 984.4 cm^{-1} band is due to the sulphate bonded to water and the 987.7 cm^{-1} band attributed to sulphate bonded to the divalent cation. The Raman spectra at 77 K imply three different non-equivalent sulphate units. X-ray diffraction at low temperatures would be needed to prove this concept. From a spectroscopic point of view, the situation is complex, since all these isomorphous minerals crystallise in a monoclinic space group $P 2_1/c$ and four independently sulphate ions are present. In the unit cell, there are 16 anions in the primitive cell each located in the C_1 position. So additional numerous bands due to crystal effects are expected. There are four crystallographically independent sulphate ions. This will result in numerous band splittings, which are more readily observed at 77K. Hence it would be expected that each independent sulphate anion would have its individual Raman spectrum.

The infrared spectrum of [Figure 1](#) shows a broad profile with three bands observed at 1055.9 , 1107.0 and 1138.1 cm^{-1} . These bands are assigned to the ν_3 antisymmetric stretching vibrations. Ross reported two infrared bands for pickeringite at 1085 and 1025 cm^{-1} and three bands for halotrichite at 1121 , 1085 and 1068 cm^{-1} [11]. In the Raman spectrum at 298 K two bands are observed at 1084.1 and 1146.5 cm^{-1} and are attributed to the sulphate antisymmetric stretching vibrations. Four bands are observed in this region in the 77 K spectrum at 1052.1 , 1076.5 , 1115.4 and 1146.5 cm^{-1} . There are two different types of sulphates in the structure of

halotrichite and it would be expected that two sets of antisymmetric stretching bands would be obtained. Thus in correspondence with the two symmetric stretching bands at 77 K, two sets of bands are obtained. One set is 1052.1 and 1115.4 cm^{-1} and the second set 1076.5 and 1146.5 cm^{-1} .

The low wavenumber regions of halotrichite at 298 and 77K are shown in **Figure 2**. The Raman spectrum of the ν_2 region of halotrichite at 298 K shows two bands at 445.1 and 466.9 cm^{-1} . In the 77 K spectrum four bands are found at 435.2, 466.7, 481.7 and 534.1 cm^{-1} . A previous study showed halotrichite showed two bands at 468 and 424 cm^{-1} for halotrichite [13]. Halotrichites are known for forming a continuous solid solution with pickeringite. This results from the substitution of Mg^{2+} for Fe^{2+} . In some ways this means that every example of halotrichite may be of a different composition and may give different Raman spectra. Ross reported one infrared band for halotrichite at 480 cm^{-1} and a band for pickeringite at 435 cm^{-1} [11]. The infrared spectrum shows a broad band at 572.1 cm^{-1} which is ascribed to the sulphate ν_4 bending mode. In the Raman spectrum at 298 K two bands are found at 605.5 and 624.2 cm^{-1} . Ross reports two ν_4 modes in the infrared spectra at 645 and 600 cm^{-1} for halotrichite and 638 and 600 cm^{-1} for pickeringite [11]. The infrared spectra of halotrichite show two bands at 612 and 572 cm^{-1} . The Raman spectrum at liquid nitrogen temperature shows better band separation and bands are observed at 593.5, 606.9, 620.7 and 633.3 cm^{-1} . Some sulphates have their symmetry reduced through the formation of monodentate and bidentate ligands. In the case of bidentate formation both bridging and chelating ligands are known. This reduction in symmetry is observed by the splitting of the ν_3 and ν_4 into two components under C_{3v} symmetry and into 3 components under C_{2v} symmetry. The observation that 3 or 4 bands are observed in the ν_4 region of halotrichites is attributed to the reduction of symmetry to C_{2v} or less, and the fact that four crystallographically distinct sulphate groups are present in the structure, one acts as a unidentate towards the M^{2+} ion.

The Raman spectrum of halotrichite in the 2800 to 3800 cm^{-1} region is shown in **Figure 3**. The infrared spectrum displays four bands at 3239.0, 3371.4, 3485.7 and 3569.5 cm^{-1} . Some selected studies have shown a strong correlation between OH stretching frequencies and both the O \cdots O bond distances and the H \cdots O hydrogen bond distances. [18-21] The elegant work of Libowitzky (1999) showed that a regression function can be employed relating the above correlations with regression coefficients better than 0.96 [22]. The function is $\nu_1 = 3592 - 304 \times 10^9 \exp(-d(\text{O}-\text{O})/0.1321)$ cm^{-1} . Two types of OH units are identified in the structure and the known hydrogen bond distances used to predict the hydroxyl stretching frequencies. By using the band positions of the OH stretching bands in the infrared spectrum hydrogen bond distances using the formula above can be calculated. The values obtained are 2.718 Å (3239 cm^{-1}), 2.780 Å (3371.4 cm^{-1}), 2.876 Å (3485.7 cm^{-1}) and 3.081 Å (3569.5 cm^{-1}). The hydroxyl stretching modes of weak hydrogen bonds occur in the 3580–3500 cm^{-1} region and the hydroxyl stretching modes of strong hydrogen bonds occurs below 3485 cm^{-1} . When the water is coordinated to the cation in the clays as occurs in certain minerals, then the water OH stretching frequency occurs at 3220 cm^{-1} . A simple observation can be made that as the water OH stretching frequency decreases then the HOH bending frequency increases. The 3239 cm^{-1} band corresponds to an ice-like structure with O-H \cdots O bond distances of 2.718 Å. In the infrared spectrum of halotrichite a strong band is found at 1647 cm^{-1} . The Raman band is observed at 1662 cm^{-1} at 298 K and at 1650 cm^{-1} at 77 K. The water hydroxyl stretching and the water

HOH bending 1610 cm^{-1} frequencies provide a measure of the strength of the bonding of the water molecules. Likewise the position of the water bending vibration also provides a measure of this strength of water hydrogen bonding. Bands that occur at frequencies above 1650 cm^{-1} are indicative of coordinated water and chemically bonded water. Bands that occur below 1630 cm^{-1} are indicative of water molecules that are not as tightly bound. In this case the hydrogen bonding is weaker as the frequency decreases

Conclusions

Halotrichites are a pseudo alum which can form a continuous series of solid solutions with pickingerite by the substitution of Mg for Fe^{2+} . Raman spectroscopy is a very powerful tool for the study of these types of minerals and because of the compositional variation differences in the Raman spectrum of halotrichites of different origins are observed. The crystal structure of halotrichites shows four non-equivalent sulphate units, three of which are bonded to water molecules and one to the divalent cation. Raman spectroscopy identifies two sulphate symmetric stretching vibrations in line with the crystal structure. At 77 K, three bands are observed implying that some structural change in the halotrichite occurs on reaching 77 K. Multiple antisymmetric stretching bands are observed as well as multiple bending modes suggesting a reduction in symmetry of the sulphate in the halotrichite structure. The variation in the Raman spectrum of halotrichite with increasing substitution of Fe^{2+} by Mg needs to be further explored.

Acknowledgments

The financial and infra-structure support of the Queensland University of Technology Inorganic Materials Research Program of the School of Physical and Chemical Sciences is gratefully acknowledged. The Australian Research Council (ARC) is thanked for funding.

References

- [1]. J. Uhlig, *Centr. Min.* (1912) 723.
- [2]. F. Wirth, *Angewandte Chem.* 26 (1913) 81.
- [3]. Y. N. Neradovskii, A. N. Bogdanova, G. M. Neradovskaya and R. A. Popova, *Zapiski Vsesoyuznogo Mineralogicheskogo Obshchestva* 108 (1979) 343.
- [4]. J. L. Jambor, D. K. Nordstrom and C. N. Alpers, *Rev. Min. Geochem.* 40 (2000) 303.
- [5]. R. G. Corbett, E. B. Nuhfer and H. W. Phillips, *Proceedings of the West Virginia Academy of Science* 39 (1967) 311.
- [6]. R. Martin, K. A. Rodgers and P. R. L. Browne, *Min. Mag.* 63 (1999) 413.
- [7]. A. D. Cody and T. R. Grammer, *New Zealand J. Geol. Geophys.* 22 (1979) 495.
- [8]. M. C. Brandy, *Am. Min.* 23 (1938) 669.
- [9]. C. Palache, H. Berman, C. Frondel and Editors, *Dana's System of Mineralogy. Vol. II. 7th ed*, 1951.
- [10]. S. Menchetti and C. Sabelli, *Min. Mag.* 40 (1976) 599.
- [11]. S. D. Ross, in *The infrared spectra of minerals*, Chapter 18 pp 423 (1974) The Mineralogical Society, London.
- [12]. S. D. Ross, *Inorganic Infrared and Raman Spectra (European Chemistry Series)*, 1972.
- [13]. R. L. Frost, J. T. Kloprogge, P. A. Williams and P. Leverett, *J. Raman. Spec.* 31 (2000) 1083.
- [14]. R. L. Frost, *Anal. Chim. Acta* 517 (2004) 207.
- [15]. R. L. Frost, J. T. Kloprogge and W. N. Martens, *J. Raman. Spec.* 35 (2004) 28.
- [16]. R. L. Frost and M. L. Weier, *J. Raman. Spec.* 35 (2004) 299.
- [17]. R. L. Frost, P. A. Williams, W. Martens, P. Leverett and J. T. Kloprogge, *Am. Min.* 89 (2004) 1130.
- [18]. J. Emsley, *Chem. Soc. Rev.* 9 (1980) 91.
- [19]. H. Lutz, *Structure and Bonding (Berlin, Germany)* 82 (1995) 85.
- [20]. W. Mikenda, *J. Mol. Struct.* 147 (1986) 1.
- [21]. A. Novak, *Structure and Bonding* 18 (1974) 177.
- [22]. E. Libowitzky, *Monatshefte für chemie* 130 (1999) 1047.

Table 1 Results of the Infrared and Raman spectra of halotrichite

ATR-IR			298K Raman			77K Raman		
Centre	FWHM	%	Centre	FWHM	%	Centre	FWHM	%
3569.5	72.9	0.5				3565.1	29.3	0.7
3485.7	150.7	1.2	3545.5	110.5	2.1	3498.0	21.8	0.4
			3425.4	146.5	29.1	3412.8	55.5	3.2
3371.4	89.1	0.5				3412.3	231.4	20.2
3239.0	349.7	25.4	3269.1	232.2	31.9	3249.2	107.1	7.0
						3189.9	245.2	22.7
2906.8	373.6	26.7				2958.2	207.9	13.3
2484.2	363.4	10.2						
1646.8	74.9	2.8	1662.0	83.1	0.9	1650.9	91.7	0.9
1597.6	152.3	2.3	1568.2	73.2	0.1			
1455.9	151.7	0.9						
1138.1	46.1	1.3	1146.5	27.1	2.9	1146.5	33.4	1.2
1107.0	28.4	2.1				1115.4	20.7	1.1
			1084.1	41.9	3.0	1076.5	32.1	1.8
1055.9	73.4	16.1				1052.1	10.9	0.2
1042.5	18.3	0.5						
						1000.0	5.9	7.3
992.7	9.6	0.2	987.7	22.1	3.1	991.3	6.6	4.3
			984.4	4.7	12.3	985.0	4.3	0.9
			983.1	22.4	2.0			
981.0	12.7	0.2	981.9	4.6	2.9	971.8	20.1	5.3
950.7	29.5	0.7						
947.2	96.6	5.4						
						880.1	25.0	0.4
744.7	45.4	0.3						
704.5	47.6	0.7						
						633.3	53.9	1.0
			624.2	34.9	1.1	620.7	20.1	1.3
612.3	14.0	0.1	605.5	54.9	3.0	606.9	7.5	0.3
						593.5	21.7	0.4
572.1	75.9	2.1						
						534.1	10.8	0.2
						481.7	15.1	0.5
			466.9	17.9	1.9	466.7	25.4	2.9
			445.1	21.9	1.2	435.2	12.5	0.1
			422.1	14.2	0.1	424.2	9.7	0.8
			380.1	25.5	0.2			
			361.5	21.3	0.4	353.7	7.4	0.1
						317.3	10.6	0.4
						301.9	7.3	0.1
						264.4	5.9	0.0
			244.6	28.6	0.9	247.2	17.9	0.4
			220.5	23.0	0.7	227.1	13.5	0.4
			204.2	11.5	0.2	199.3	13.7	0.1

	181.8	6.8	0.0	185.9	9.5	0.1
	116.0	1.6	0.0	163.1	7.1	0.1

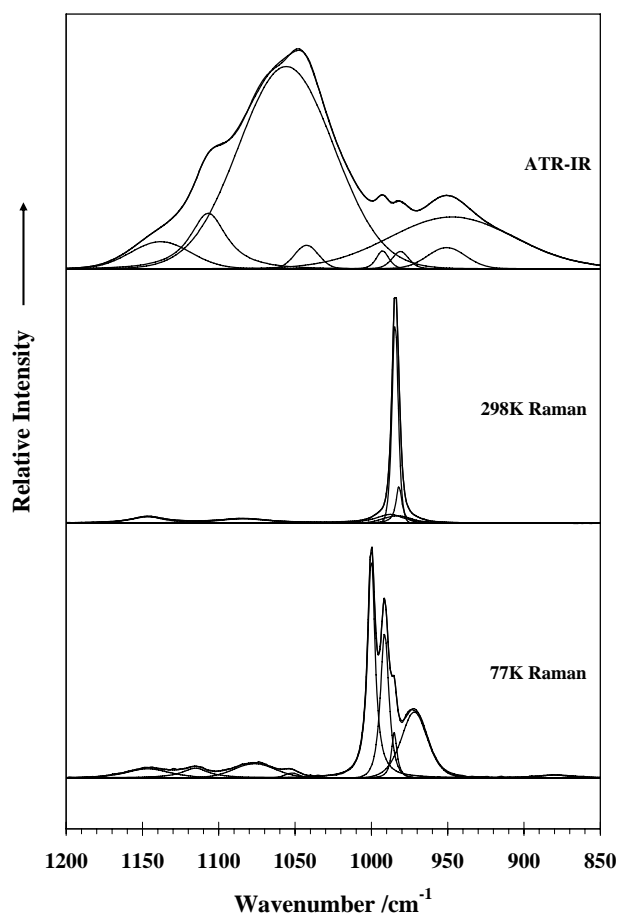


Figure 1

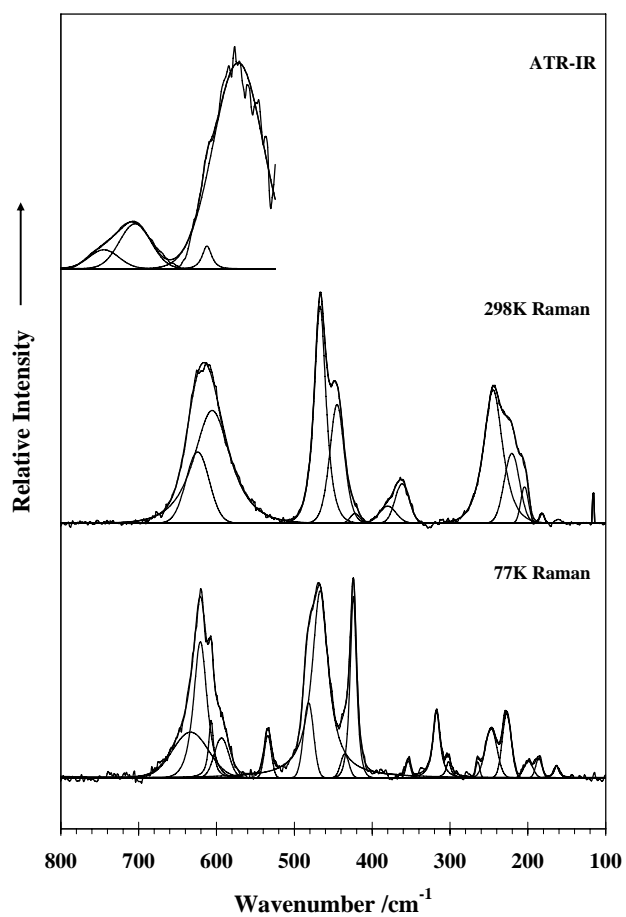


Figure 2

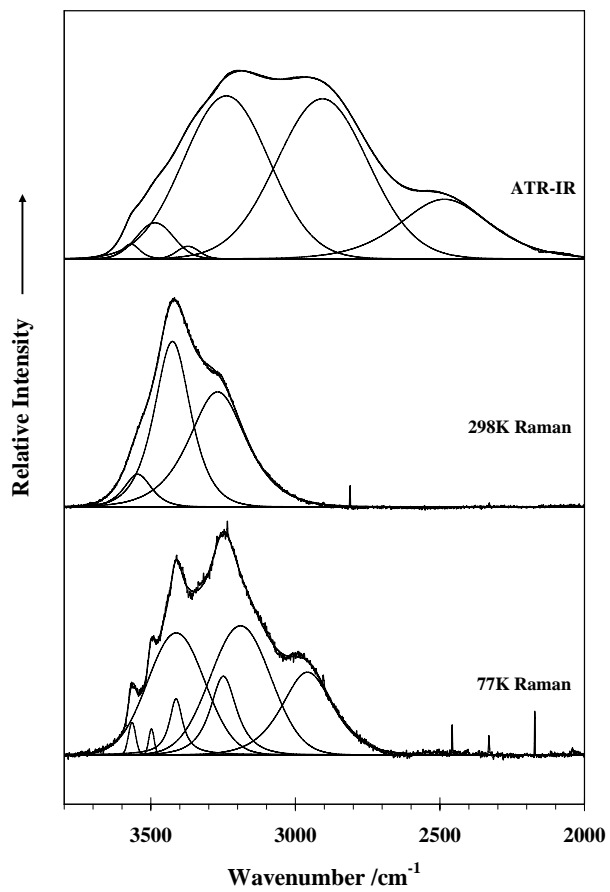


Figure 3

